

GMPR: A robust normalization method for zero-inflated count data with application to microbiome sequencing data

Li Chen¹, **James Reeve**², **Lujun Zhang**³, **Shengbing Huang**², **Xuefeng Wang**⁴, **Jun Chen**^{Corresp. 2, 5}

¹ Department of Health Outcomes Research and Policy, Harrison School of Pharmacy, Auburn University, Auburn, Alabama, United States

² Bioinformatics and Computational Biology Program, University of Minnesota - Rochester, Rochester, Minnesota, United States

³ College of Environmental and Resource Sciences, Zhejiang University, Hangzhou, Zhejiang, China

⁴ Department of Biostatistics and Bioinformatics, Moffitt Cancer Center, Tampa, Florida, United States

⁵ Division of Biomedical Statistics and Informatics and Center for Individualized Medicine, Mayo Clinic, Rochester, Minnesota, United States

Corresponding Author: Jun Chen

Email address: chen.jun2@gmail.com

Normalization is the first critical step in microbiome sequencing data analysis used to account for variable library sizes. Current RNA-Seq based normalization methods that have been adapted for microbiome data fail to consider the unique characteristics of microbiome data, which contain a vast number of zeros due to the physical absence or under-sampling of the microbes. Normalization methods that specifically address the zero inflation remain largely undeveloped. Here we propose GMPR - a simple but effective normalization method - for zero-inflated sequencing data such as microbiome data. Simulation studies and real datasets analyses demonstrate that the proposed method is more robust than competing methods, leading to more powerful detection of differentially abundant taxa and higher reproducibility of the relative abundances of taxa.

1 **GMPR: A robust normalization method for** 2 **zero-inflated count data with application to** 3 **microbiome sequencing data**

4 **Li Chen¹, James Reeve², Lujun Zhang³, Shengbing Huang², Xuefeng**
5 **Wang⁴, and Jun Chen^{2, 5}***

6 ¹**Department of Health Outcomes Research and Policy, Harrison School of Pharmacy,**
7 **Auburn University, AL 36849, USA**

8 ²**Bioinformatics and Computational Biology Program, University of Minnesota,**
9 **Rochester, MN 55905, USA**

10 ³**College of Environmental and Resource Sciences, Zhejiang University, Zhejiang,**
11 **310058, China**

12 ⁴**Department of Biostatistics and Bioinformatics, Moffitt Cancer Center, Tampa, FL**
13 **33612, USA**

14 ⁵**Division of Biomedical Statistics and Informatics and Center for Individualized**
15 **Medicine, Mayo Clinic, Rochester, MN 55905, USA**

16 ***Corresponding addressed to: Chen.Jun2@mayo.edu**

17 **ABSTRACT**

18 Normalization is the first critical step in microbiome sequencing data analysis used to account for variable
19 library sizes. Current RNA-Seq based normalization methods that have been adapted for microbiome
20 data fail to consider the unique characteristics of microbiome data, which contain a vast number of
21 zeros due to the physical absence or under-sampling of the microbes. Normalization methods that
22 specifically address the zero-inflation remain largely undeveloped. Here we propose GMPR - a simple but
23 effective normalization method - for zero-inflated sequencing data such as microbiome data. Simulation
24 studies and real datasets analyses demonstrate that the proposed method is more robust than competing
25 methods, leading to more powerful detection of differentially abundant taxa and higher reproducibility of
26 the relative abundances of taxa.

27 **INTRODUCTION**

28 High-throughput sequencing experiments such as RNA-seq and microbiome sequencing are now routinely
29 employed to interrogate the biological systems at the genome scale (Wang et al., 2009). After processing
30 of the raw sequence reads, the sequencing data usually presents as a count table of detected features. The
31 complex processes involved in the sequencing causes the sequencing depth (library size) to vary across
32 samples, sometimes ranging several orders of magnitude. Normalization, which aims to correct or reduce
33 the bias introduced by variable library sizes, is an essential preprocessing step before any downstream
34 statistical analyses for high-throughput sequencing experiments (Dillies et al., 2013; Li et al., 2015).
35 Normalization is especially critical when the library size is a confounding factor that correlates with the
36 variable of interest. An inappropriate normalization method may either reduce statistical power with the
37 introduction of unwanted variation, or more severely, result in falsely discovered features. One popular
38 approach for normalizing the sequencing data involves calculating a size factor for each sample as an
39 estimate of the library size. The size factors can be used to divide the read counts to produce normalized
40 data (in the form of relative abundances), or to be included as offsets in count-based regression models
41 such as DESeq2 (Love et al., 2014) and edgeR (Robinson et al., 2010) for differential feature analysis.
42 One simple normalization method is TSS (Total Sum Scaling), which uses the total read count for each
43 sample as the size factor. However, there are a couple undesirable properties for TSS. First, it is not robust
44 to outliers, which are disproportionately large counts that do not reflect the underlying true abundance.
45 Outliers have frequently been observed in sequencing samples due to technical artifacts such as preferential

46 amplification by PCR (Aird et al., 2011). Several outliers could lead to the overestimation of the library
47 size if not properly addressed. Second, it creates compositional effects: non-differential features will
48 appear to be differential due to the constant-sum constraint (Tsilimigras and Fodor, 2016; Mandal et al.,
49 2015; Morton et al., 2017). Compositional effects are much stronger when the differential features are
50 highly abundant or their effects are in the same direction (not balanced). An ideal normalization method
51 should thus capture the invariant part of the count distribution and be robust to outliers and differential
52 features.

53 Many normalization methods have been developed for sequencing data generally, and for RNA-Seq
54 data in particular (Dillies et al., 2013; Li et al., 2015). These methods mostly rely on the assumption that
55 the dataset to be normalized has a large invariant part and the majority of features do not change with
56 respect to the condition under study. Robust statistics such as median and trimmed mean, which are not
57 sensitive to a small set of differential features, are frequently used to estimate the library size. Two popular
58 normalization methods for RNA-Seq data include TMM (Trimmed Mean of M values, implemented
59 in edgeR) (Robinson and Oshlack, 2010) and the DESeq normalization (equivalent to Relative Log
60 Expression normalization implemented in edgeR. For simplicity, we label it as “RLE”.) (Anders and
61 Huber, 2010). RLE method calculates the geometric means of all features as a “reference”, and all
62 samples are compared to the “reference” to produce ratios (fold changes) for all features. The median
63 ratio is then taken to be the RLE size factor. TMM method, on the other hand, selects a reference sample
64 first, and all other samples are compared to the reference sample. The trimmed (weighted) mean of the
65 log ratios is then calculated as the TMM size factor (log scale). Compared to RNA-Seq data, microbiome
66 sequencing data are more over-dispersed and contain a vast number of zeros. For example, the human
67 fecal microbiome data set from a study of the long-term dietary effect on the gut microbiota (“COMBO”
68 data) contains 1,873 non-singleton OTUs (Operational Taxonomic Units, a proxy for bacterial species)
69 from 99 subjects and more than 80% of the OTU counts are zeros (Wu et al., 2011). Excessive zeros lead
70 to a small number of “core” OTUs that are shared across samples. For the COMBO dataset, none of the
71 OTUs are shared by all samples and only 5 OTUs are shared by more than 90% samples. For RLE, the
72 geometric means of OTUs are not well defined for OTUs with 0s, and OTUs with 0s are typically excluded
73 in size factor calculation. We are thus left with a very small number of common OTUs to calculate the
74 size factor. As the OTU data become more sparse, RLE becomes less stable. For datasets like COMBO
75 data, where there are no common OTUs, RLE fails. For TMM, a reference sample has to be selected
76 before the size factor calculation. Reliance on a reference sample restricts the size factor calculation to a
77 specific OTU set that the reference sample harbors (77 – 433 OTUs for COMBO data). Therefore, both
78 RLE and TMM use only a small fraction of the data available in the OTU data and are not optimal from
79 an information perspective.

80 One popular strategy to circumvent the zero-inflation problem is to add a pseudo-count (Mandal et al.,
81 2015). This practice has a Bayesian explanation and implicitly assumes that all the zeros are due to
82 under-sampling (McMurdie and Holmes, 2014). However, this assumption may not be appropriate due to
83 the large extent of structural zeros due to physical absence. Moreover, the choice of the pseudo-count is
84 very arbitrary and it has been shown that the clustering results can be highly dependent upon the choice
85 (Costea et al., 2014). Recently, a new normalization method CSS (Cumulative Sum Scaling) has been
86 developed for microbiome sequencing data (Paulson et al., 2013). In CSS, raw counts are divided by the
87 cumulative sum of counts, up to a percentile determined using a data-driven approach. The percentile
88 is aimed to capture the relatively invariant count distribution for a dataset. However, the determination
89 of the percentiles could fail for microbiome datasets that have high count variability. Therefore, a more
90 robust method to address the zero-inflated sequencing data is still needed.

91 Here we propose a novel inter-sample normalization method GMPR (Geometric Mean of Pairwise
92 Ratios), developed specifically for zero-inflated sequencing data such as microbiome sequencing data. By
93 comprehensive tests on simulated and real datasets, we show that GMPR outperforms the other competing
94 methods for zero-inflated count data.

95 METHODS

96 GMPR normalization details

97 Our method extends the idea of RLE normalization for RNA-seq data and relies on the same assumption
98 that there is a large invariant part in the count data. Assume we have a count table of OTUs from 16S
99 rDNA targeted microbiome sequencing. Denote the c_{ki} as the count of the k th OTU ($k = 1, \dots, q$) in the

100 i th ($i = 1, \dots, n$) sample. The RLE method calculates the size factor s_i , which estimates the (relative)
 101 library size of a given sample, based on

- Step 1: Calculate the geometric means for all OTUs

$$\mu_k^{GM} = (c_{k1}c_{k2} \cdots c_{kn})^{1/n}, k = 1, \dots, q$$

- Step 2: For a given sample,

$$s_i = \text{median}_k \{c_{ki}/\mu_k^{GM}\}, i = 1, \dots, n$$

Since geometric mean is not well defined for features with 0s, features with 0s are usually excluded in size calculation. However, for zero-inflated data such as microbiome sequencing data, as the sample size increases, the probability of existence of features without any 0s becomes smaller. It is not uncommon that a large dataset does not share any common taxa. In such cases, RLE fails. As an alternative, a pseudo-count such as 1 or 0.5 has been suggested to add to the original counts to eliminate 0s (Mandal et al., 2015). Since the majority of the counts may be 0s for microbiome data, adding even a small pseudo-count could have a dramatic effect on the geometric means of most OTUs. To circumvent the problem, GMPR reverses the order of the two steps of RLE. The first step is to calculate r_{ij} , which is the median count ratio of nonzero counts between sample i and j ,

$$r_{ij} = \underset{k \in \{1, \dots, q\} | c_{ki} \cdot c_{kj} \neq 0}{\text{Median}} \left\{ \frac{c_{ki}}{c_{kj}} \right\},$$

The second step is to calculate the size factor s_i for a given sample i as

$$s_i = \left(\prod_{j=1}^n r_{ij} \right)^{1/n}, i = 1, \dots, n.$$

102 Figure 1 illustrates the procedure of GMPR. The basic strategy of GMPR is that we conduct the
 103 pairwise comparison first and then combine the pairwise results to obtain the final estimate. Although
 104 only a small number of OTUs (or none) are shared across all samples due to severe zero-inflation, for
 105 every pair of samples, they usually share many OTUs. For example, 83 OTUs are shared on average
 106 for COMBO sample pairs. Thus, for pairwise comparison, we focus on these common OTUs that are
 107 observed in both samples to have a reliable inference of the abundance ratio between samples. We then
 108 synthesize the pairwise abundance ratios using a geometric mean to obtain the size factor. Based on this
 109 pair analysis strategy, we utilize far more information than RLE and TMM, both of which are restricted to
 110 a small subset of OTUs. It should be noted that GMPR is a general method, which could be applied to
 111 any type of sequencing data in principle.

112 The R implementation of GMPR could be accessed by [https://github.com/jchen1981/](https://github.com/jchen1981/GMPR)
 113 GMPR.

114 Simulation studies to evaluate the performance of GMPR normalization

115 We study the performance of GMPR using simulated OTU datasets. Specifically, we study the robustness
 116 of GMPR to differential and outlier OTUs, and the effect on the performance of differential abundance
 117 analysis of OTU data. We compare GMPR to competing normalization methods including CSS, RLE,
 118 RLE+ (RLE with pseudo-count 1), TMM, TMM+ (TMM with pseudo-count 1) and TSS. The details of
 119 calculating the size factors using each normalization method are described in Box 1. The size factors
 120 from different normalization methods are further divided by the median so that they are on the same scale.

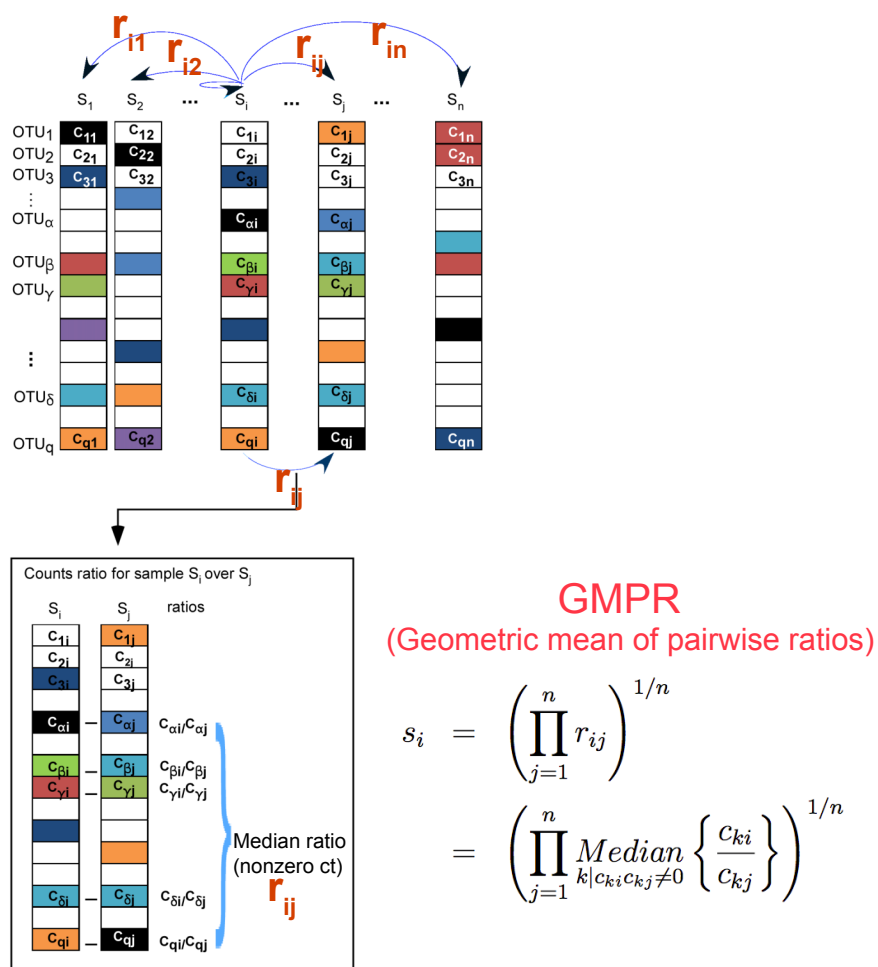


Figure 1. GMPR starts with pairwise comparisons (upper). Each pairwise comparison calculates the median abundance ratio of those common OTUs between the pair of samples (lower). The pairwise ratios are then synthesized into a final estimate.

Box 1. Calculation of size factors for normalization methods compared in the analysis.

- **GMPR (Geometric Mean of Pairwise Ratios):** The size factors for all samples are calculated by GMPR described in the Method section.
- **CSS (Cumulative Sum Scaling):** The size factors for all samples are calculated by applying `newMRexperiment`, `cumNorm` and `normFactors` in Bioconductor package `metagenome-Seq` (Paulson et al., 2013).
- **RLE (Relative Log Expression):** The size factors for all samples are calculated by the `calcNormFactors` with the parameter set as “RLE” in the edgeR Bioconductor package (Anders and Huber, 2010). The scaled size factors are obtained by multiplying the size factors with the total read count.
- **RLE+ (Relative Log Expression plus pseudo-counts):** The scaled size factors for all samples are calculated in the same way as RLE, except that each data entry is added with a pseudo-count 1.
- **TMM (Trimmed Mean of M values):** The size factors for all samples are calculated by the `calcNormFactors` function with the parameter set as “TMM” in the edgeR Bioconductor package (Robinson and Oshlack, 2010). The scaled size factors are obtained by multiplying the size factors with the total read count.
- **TMM+ (Trimmed Mean of M values plus pseudo-counts):** The scaled size factors for all sample are calculated in the same way as TMM, except that each data entry is added with a pseudo-count 1.
- **TSS (Total Sum Scaling):** The size factors are taken to be the total read counts.

121

122 Robustness to differential and outlier OTUs

123 We first use a perturbation-based simulation approach to evaluate the performance of normalization
 124 methods, focusing on their robustness to differentially abundant OTUs and sample-specific outlier OTUs.
 125 The idea is that we first simulate the counts from a common probabilistic distribution so that the total
 126 count is a proxy of the “true” library size. Next, we perturb the counts in different ways and apply
 127 different normalization methods on the perturbed counts and evaluate the performance based on the
 128 correlation between estimated size factor and “true” library size. Specifically, we generate zero-inflated
 129 count data based on a Dirichlet-multinomial model with known library sizes (Chen and Li, 2013). The
 130 mean and dispersion parameters of Dirichlet-multinomial distribution are estimated from the COMBO
 131 dataset after filtering out rare OTUs with less than 10 reads and discarding samples with less than 1,000
 132 reads ($n=98, q=625$) (Wu et al., 2011). The library sizes are also drawn from those of the COMBO data.
 133 To investigate the effect of sparsity (the number of zeros), OTU counts are simulated with different zero
 134 percentages ($\sim 60\%$, 70% and 80%) by adjusting the dispersion parameter. A varying percentage of OTUs
 135 (0% , 1% , 2% , 4% , 8% , 16% , 32% , 64%) are perturbed in each set of simulation, with varying strength of
 136 perturbation. The counts c_{ki} of perturbed OTUs are changed to $\sqrt{c_{ki}}$ or c_{ki}^2 for strong perturbation and
 137 $0.25c_{ki}$ or $4c_{ki}$ for moderate perturbation.

138 We employ two perturbation approaches where we decrease/increase the abundances of a “fixed” or
 139 “random” set of OTUs. As shown in Figure 2, in the “fixed” perturbation approach, the same set of OTUs
 140 are decreased/increased in the same direction for all samples, reflecting differentially abundant OTUs
 141 under a certain condition such as disease state. In the “random” perturbation approach, each sample has a
 142 random set of OTUs perturbed with a random direction, mimicking the sample-specific outliers.

143 Finally, size factors for all methods are estimated and the Pearson’s correlation between the estimated
 144 and “true” library sizes is calculated. The simulation is repeated 25 times and the mean estimate and its
 145 95% confidence intervals (CIs) are reported.

146 Effect on the performance of differential abundance analysis

147 One use of the estimated size factor is for differential abundance analysis (DAA) of OTU data, where
 148 the size factor (usually on a log scale) is included as an offset in a count-based parametric model to
 149 address variable library sizes. Many count-based models have been proposed for differential abundance
 150 analysis including DESeq2 and edgeR (McMurdie and Holmes, 2014). These methods usually come
 151 with their native normalization schemes such as RLE for DESeq2 and TMM for edgeR. Therefore, it

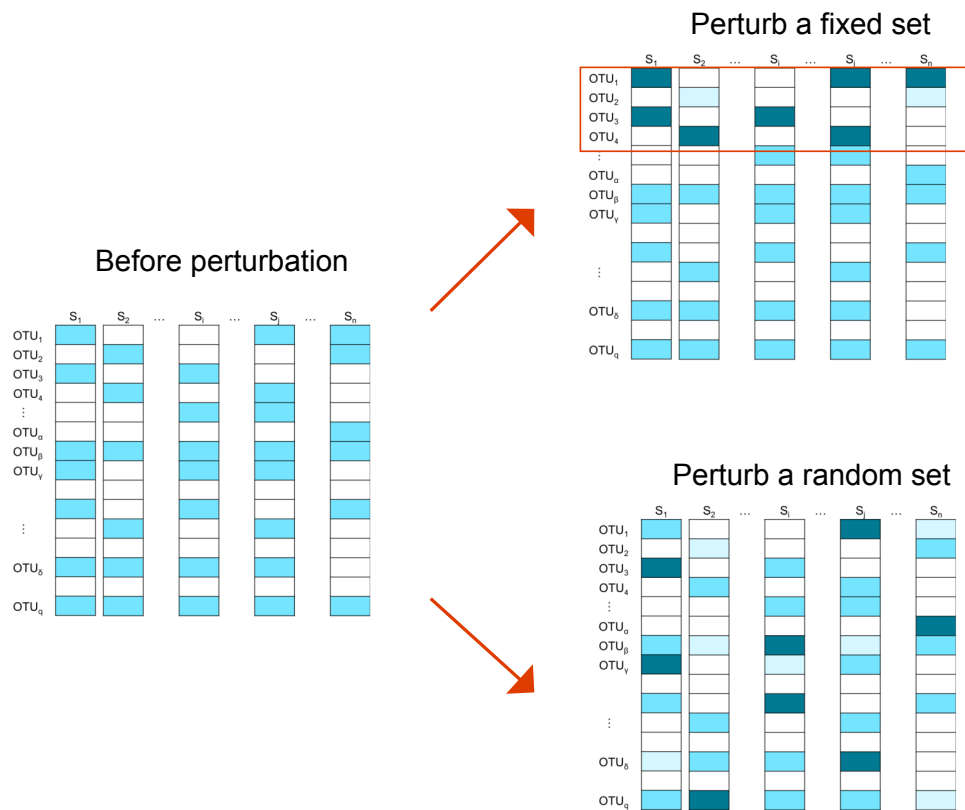


Figure 2. Illustration of the simulation strategy. In the “fixed” perturbation approach, the abundances of the same set of OTUs are decreased/increased for all samples, reflecting differentially abundant OTUs under certain conditions such as disease state. In the “random” perturbation approach, each sample has a random set of OTUs perturbed with a random direction, reflecting the sample-specific outliers. The darkness of the color indicates the OTU abundance.

152 is interesting to see if the GMPR normalization could improve the performance of these methods. To
 153 achieve this end, we use DESeq2 to perform DAA on the OTU table since DESeq2 has been shown to be
 154 more robust than edgeR for zero-inflated dataset (Chen et al., 2018). We compare the performance of
 155 DESeq2 using its native RLE normalization to that using GMPR or TSS normalization.

156 We use the same simulation strategy described in Chen et al. (2018). Specifically, Zero-inflated
 157 Negative Binomial distribution (ZINB) is used to simulate the OTU count data. ZINB has the following
 158 probability distribution function

$$f_{zinb}(c_{ki}|p_{ki}, \mu_{ki}, \phi_{ki}) = p_{ki} \cdot I_0(c_{ki}) + (1 - p_{ki}) \cdot f_{nb}(c_{ki}|\mu_{ki}, \phi_{ki}), \quad (1)$$

159 which is a mixture of a point mass at zero (I_0) and a negative binomial (f_{nb}) distribution of the form

$$f_{nb}(c_{ki}|\mu_{ki}, \phi_{ki}) = \frac{\Gamma(c_{ki} + \frac{1}{\phi_{ki}})}{\Gamma(c_{ki} + 1)\Gamma(\frac{1}{\phi_{ki}})} \cdot \left(\frac{\phi_{ki}\mu_{ki}}{1 + \phi_{ki}\mu_{ki}}\right)^{c_{ki}} \cdot \left(\frac{1}{1 + \phi_{ki}\mu_{ki}}\right)^{\frac{1}{\phi_{ki}}}. \quad (2)$$

The three parameters - prevalence(p_{ki}), abundance(μ_{ki}) and dispersion(ϕ_{ki}) - fully capture the zero-inflated and dispersed count data. We generate the simulated datasets (two sample groups of size 49 each) based on the parameter values estimated from the COMBO dataset. 5% of OTUs are randomly selected to have their counts in one group multiplied by a factor of 4. The groups in which this occurs are randomly selected and thus the abundance change is relatively “balanced”. To further study the performance under strong compositional effects, on top of the “balanced” simulation, we also select two highly abundant OTUs ($\pi = 0.168$ and 0.083 respectively) to be differentially abundant in one group. We then apply DESeq2 on the simulated datasets with RLE, GMPR and TSS normalization, where we denote DESeq2-GMPR, DESeq2-RLE, DESeq2-TSS for these three approaches. For each approach, the P-values are calculated for each OTU and corrected for multiple testing using false discovery rate (FDR) control (Benjamini-Hochberg procedure). We evaluate the performance based on FDR control and ROC analysis, where the true positive rate is plotted against false positive rate at different P-value cutoffs. The observed FDR is calculated as

$$\frac{FP}{\max(1, FP + TP)},$$

160 where FP and TP are the number of false and true positives respectively. Simulation results are averaged
 161 over 100 repetitions.

162 RESULTS

163 Simulation: GMPR is robust to differential and outlier OTUs

164 We first study the robustness of GMPR to differentially abundant OTUs and sample-specific outlier OTUs
 165 by using the perturbation-based simulation approach, where we artificially alter the abundances of a
 166 “fixed” or “random” set of OTUs under different levels of zero-inflation, percentage of perturbed OTUs
 167 and strength of perturbation.

168 In the simulation of “fixed” perturbation (Figure 3), the performance of all methods decrease in most
 169 cases with the increased zero percentage. TSS has excellent performance under moderate perturbation but
 170 performs unstably under strong perturbation (the correlation decreases steeply when the percentage of
 171 perturbed OTUs increases from 1% to 4%; after that, the correlation increases since the total sum moves
 172 closer to $\sum_k c_{ki}^2$, which is highly correlated with the original library size $\sum_k c_{ki}$). GMPR, followed by CSS,
 173 consistently outperforms the other methods when the perturbation is strong. When the perturbation is
 174 moderate, GMPR is only secondary to TSS when the percentage of zeros is high (80%) and on par with
 175 TSS when the percentage of zeros is moderate (70%) or low (60%). For RNA-Seq based methods, TMM
 176 performs better than RLE in either strong or moderate perturbation. Though the performance of RLE+
 177 improves by adding pseudo-counts to the OTU data, the size factor estimated by TMM+ merely correlates
 178 with true library size when the zero percentage is high (70% and 80%). In contrast, GMPR, together with
 179 CSS, performs stable in all cases and GMPR yields better size factor estimate than CSS.

180 In the “random” perturbation scenario (Figure 4), performance of all methods decreases with the
 181 increased zero percentage as the “fixed” scenario. Similar to the performance in “fixed” perturbation
 182 scenario, TSS has excellent performance under moderate perturbation but performs poorly under strong
 183 perturbation. When the perturbation is strong, GMPR, followed by CSS, still outperforms the other
 184 methods. RNA-Seq based methods including TMM, TMM+, RLE and RLE+ have a similar trend as in
 185 “fixed” perturbation. However, compared to “fixed” perturbation, the performance of TMM and RLE

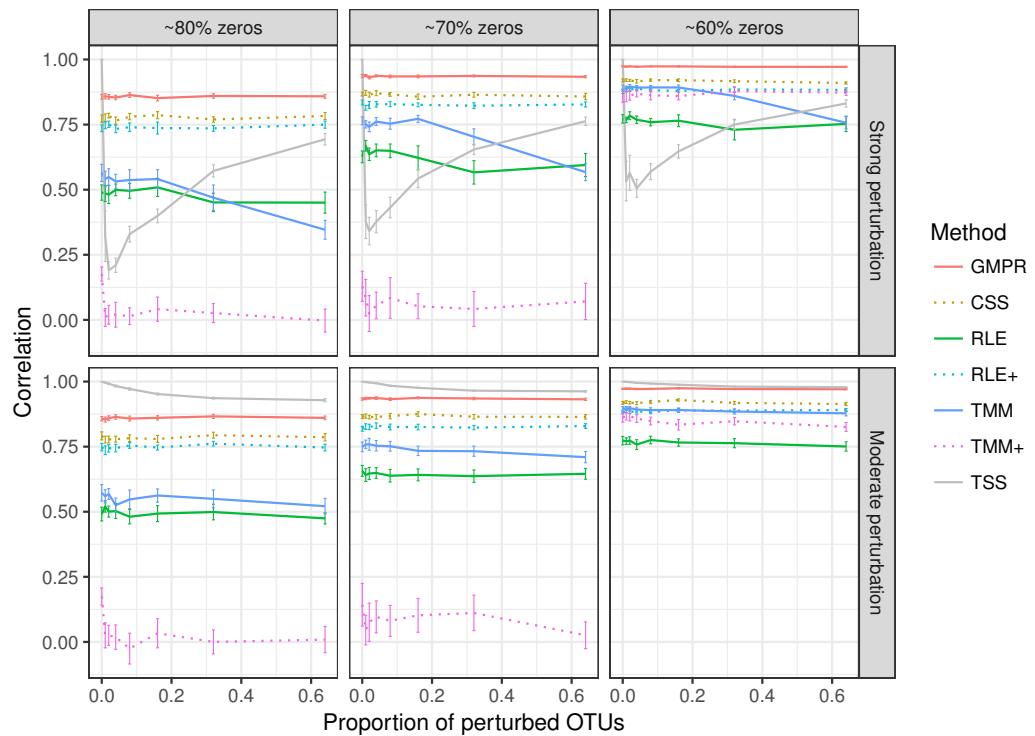


Figure 3. Spearman's correlation between the estimated size factors and the simulated "true" library sizes when a fixed set of OTUs are perturbed. The performance of different normalization methods are compared under different levels of zero-inflation, percentage of perturbed OTUs and strength of perturbation. Error bars represent 95% CIs.

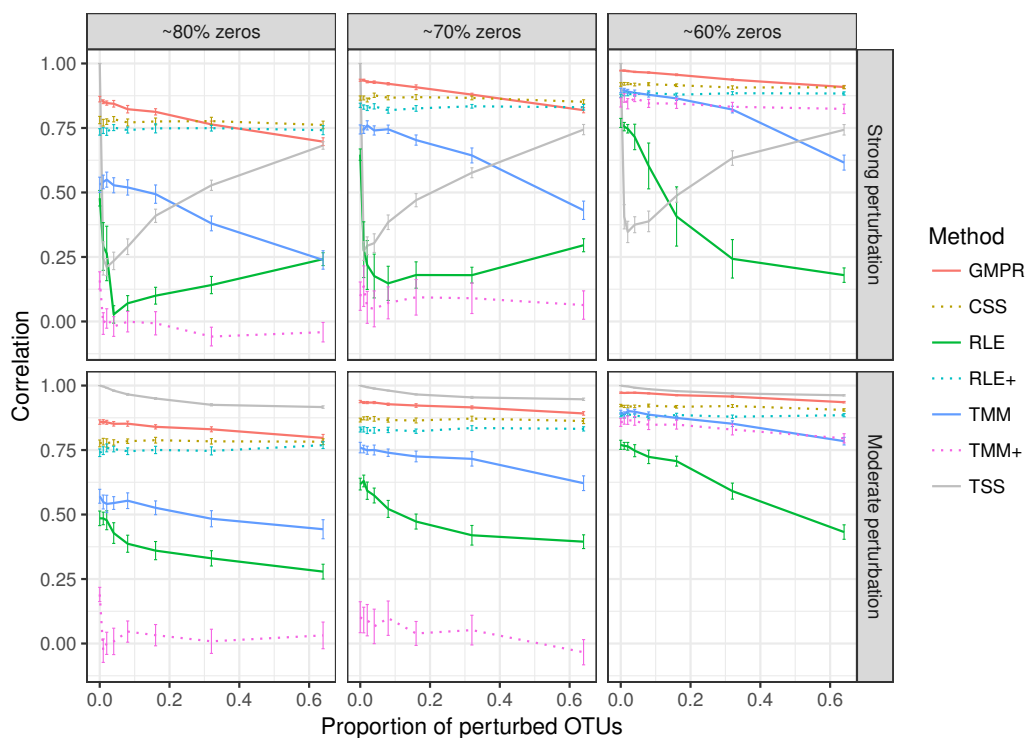


Figure 4. Spearman's correlation between the estimated size factors and the simulated "true" library sizes when a random set of OTUs are perturbed. The performance of different normalization methods are compared under different levels of zero-inflation, percentage of perturbed OTUs and strength of perturbation. Error bars represent 95% CIs.

186 decreases more obviously as the number of perturbed OTUs increases. In contrast, GMPR and CSS are
187 more robust to sample-specific outlier OTUs in all cases and GMPR results in better size factor estimate
188 than CSS.

189 **Simulation: GMPR improves the performance of differential abundance analysis**

190 In the previous section, we demonstrate that GMPR could better recover the “true” library size in
191 presence of differentially abundant OTUs or sample-specific outlier OTUs. In this section, with a different
192 perspective, we show that the robustness of GMPR method translates into a better false positive control
193 and higher statistical power in the context of differential abundance analysis (DAA), where the aim is to
194 detect differentially abundant OTUs between two sample groups.

195 We simulate the zero-inflated count data using ZINB model and use DESeq2 to perform DAA with
196 different normalization schemes (RLE, GMPR and TSS). In one scenario, we randomly select 5% OTUs
197 to be differential with a fold change of 4 in either sample group (Scene 1). In the other scenario, in
198 addition to the 5% randomly selected OTUs, we select two highly abundant OTUs to be differentially
199 abundant in one group to create strong compositional effects (Scene 2). In this scenario, the abundance
200 change of these highly abundant OTUs will lead to the change of the “relative” abundances of other
201 OTUs if the TSS normalization is used. The results for the two scenarios are presented in Figure 5. In
202 Scene 1 (Figure 5A-B), we see that all approaches have slightly elevated FDRs relative to the nominal
203 levels (Figure 5A), probably due to inaccurate P-value calculation based on the asymptotic distribution of
204 Wald statistic for those taxa with excessive zeros. Nevertheless, the observed FDR of DESeq2 using
205 GMPR is closer to the nominal level than that using RLE (native normalization) and TSS. In terms of
206 ROC-based power analysis (Figure 5B), GMPR achieves a higher AUC (Area Under the Curve) than RLE
207 and TSS. In this “balanced” scenario, TSS performs relatively well and is even slightly better than RLE.
208 The performance differences are more revealing in Scene 2 (Figure 5C-D), where we artificially alter the
209 abundances of two highly abundant OTUs. In this setting, TSS has a poor FDR control due to strong
210 compositional effects and has a much lower statistical power at the same false positive rate. In contrast,
211 the performance of GMPR and RLE remains stable, and GMPR performs better than RLE in terms of
212 both FDR control and power.

213 **Real data: GMPR reduces the inter-sample variability of normalized abundances**

214 We next evaluate various normalization methods using 38 gut microbiome datasets from 16S rDNA
215 sequencing of stool samples (Supplementary Table 1). These experimental datasets were retrieved from
216 qiita database (<https://qiita.ucsd.edu/>) with a sample size larger than 50 each. The 38 datasets come from
217 different species as well as a wide range of biological conditions. If a study involves multiple species,
218 we include samples from the predominant species. We focus the analysis on gut microbiome samples
219 because the gut microbiome is more studied than that from other sample types.

220 For the real data, it is not feasible to calculate the correlation between estimated size factors and
221 “true” library sizes as done for simulations. As an alternative, we use the inter-sample variability as
222 a performance measure since an appropriate normalization method will reduce the variability of the
223 normalized OTU abundances (raw counts divided by the size factor) due to different library sizes. A
224 similar measure has been used in the evaluation of normalization performance for microarray data (Fortin
225 et al., 2014). We use the traditional variance as the metric to assess inter-sample variability. For each
226 method, the variance of the normalized abundance of each OTU across all samples is calculated and the
227 median of the variances of all OTUs or stratified OTUs (based on their prevalence) is reported for each
228 study. For each study, all methods are ranked based on these median variances. The distributions of their
229 ranks across these 38 studies for each method are depicted in Figure 6. A higher ranking (lower values in
230 the box plot) indicates a better performance in terms of minimizing inter-sample variability.

231 In Figure 6, we could see that GMPR achieves the best performance with top ranks in 22 out of 38
232 datasets, followed by CSS, which tops in 7 datasets (Supplementary Table 2). This result is consistent
233 with the simulation studies, where GMPR and CSS are overall more robust to perturbations than other
234 methods. Moreover, GMPR consistently performs the best for reducing the variability of OTUs at different
235 prevalence levels. It is also noticeable that the inter-sample variability is the largest without normalization
236 (RAW) and TSS does not perform well for a large number of studies. As expected, RLE only works
237 for 8 out of 38 datasets due to a large percentage of zero read counts. By adding pseudo-counts, RLE+
238 improves the performance significantly compared to RLE. However, there is not much improvement of

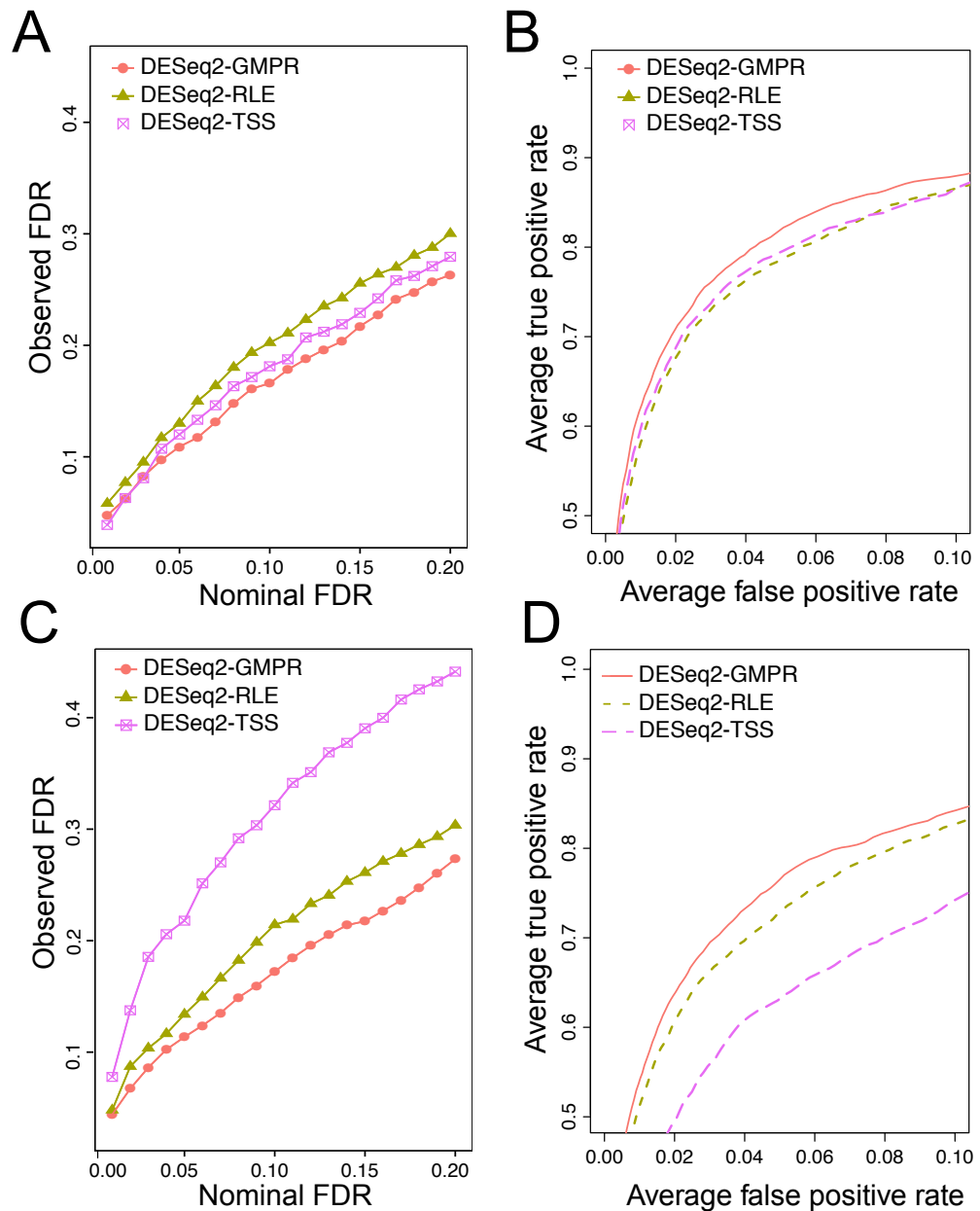


Figure 5. Comparison of the performance of different normalization schemes in DESeq2-based differential abundance analysis. A-B: Scene 1 ("balanced" scenario), 5% random OTUs are differentially abundant between two groups with a fold change of 4. C-D: Scene 2 ("unbalanced" scenario), in addition to 5% random OTUs, two highly abundant OTUs are differential abundant in one group to create strong compositional effects. A, C: ability to control the FDR. The observed FDR is plotted against the nominal FDR level. B, D: ROC curves to compare the power. The true positive rate is plotted against false positive rate at different P-value cutoffs.

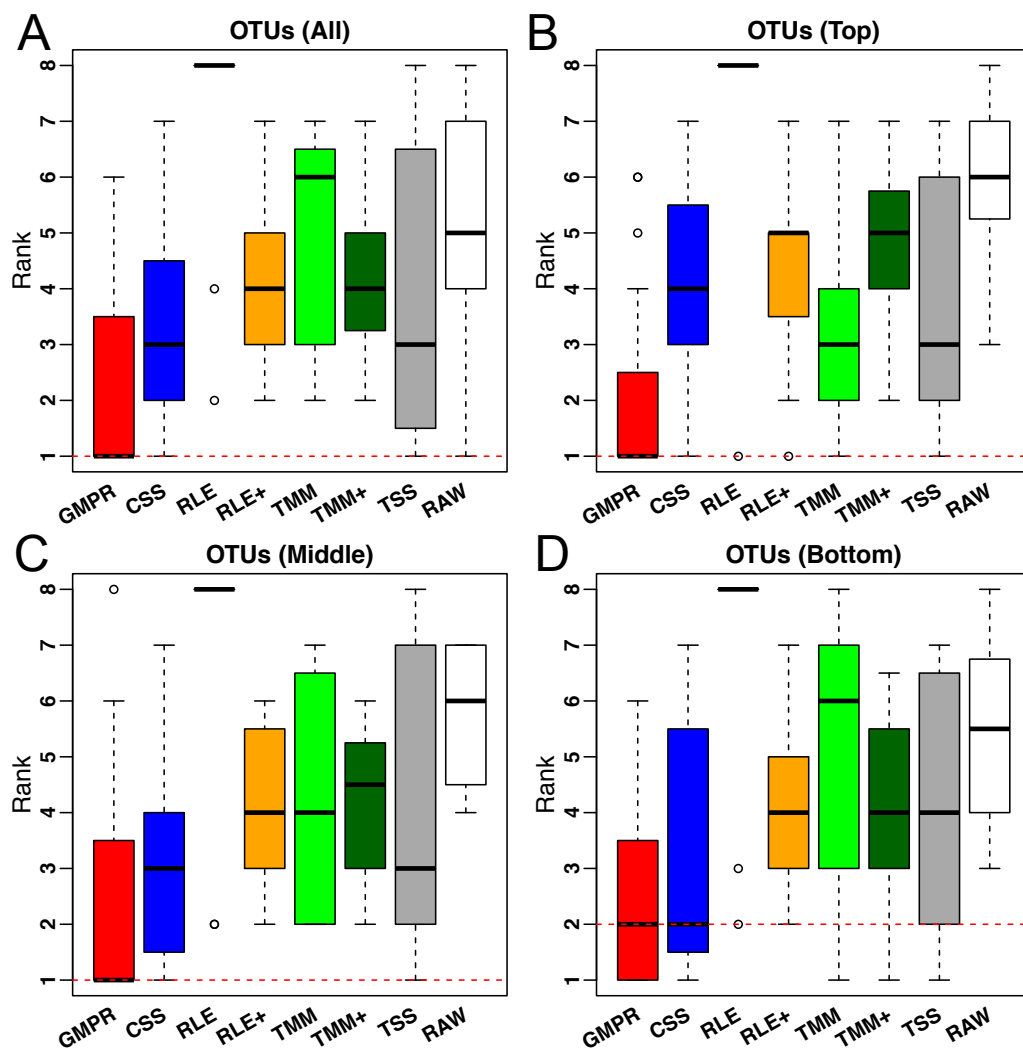


Figure 6. Comparison of normalization methods in reducing inter-sample variability of normalized OTU abundances based on 38 gut microbiome datasets. Distribution of the ranks for the medians of the OTU variances over the 38 datasets. The median is calculated over all OTUs (A) or OTUs of different prevalence level (B-C: Top, middle and bottom)

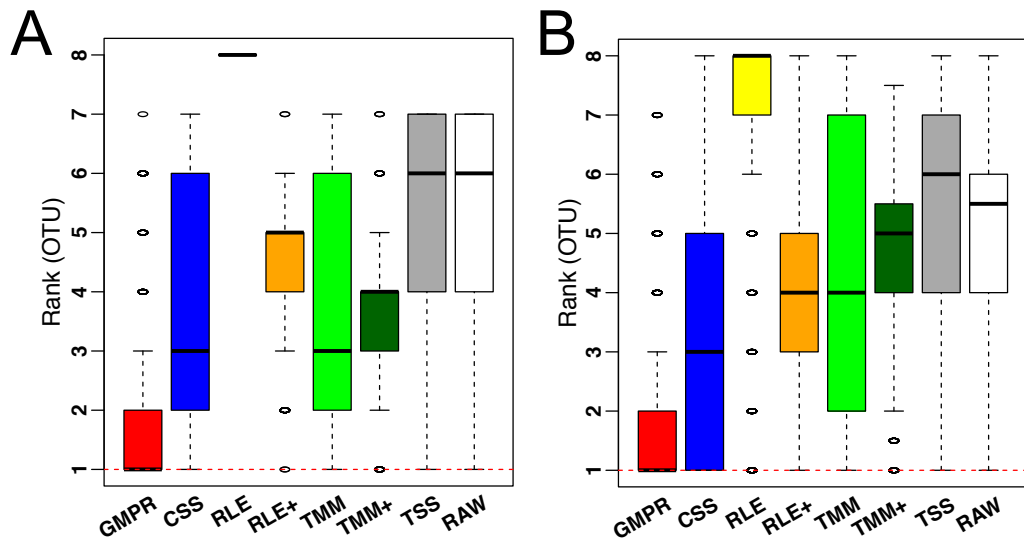


Figure 7. Comparison of normalization methods in reducing inter-sample variability of normalized OTU abundances based on an oral (A) and a skin (B) microbiome dataset. Distributions of the OTU ranks (each OTU is ranked based on its variances among the competing methods) are shown.

239 TMM+ compared to TMM. To see if the difference is significant, we performed paired Wilcoxon signed-
 240 rank tests between the ranks of the 38 datasets obtained by GMPR and by any other methods. GMPR
 241 achieves significantly better ranking than other methods (P -value <0.05 for all OTUs or stratified OTUs).
 242 Supplementary Figure 1 compares the distributions of the OTU variances and their ranks for an example
 243 dataset (study ID 1561, all OTUs). Each OTU is ranked based on its variances among the competing
 244 methods. Although the difference in median variance is moderate, GMPR performs significantly better
 245 than other methods ($P<0.05$, for all comparisons) and achieves a much lower rank.

246 To demonstrate the performance on low-diversity microbiome samples, we perform the same analyses
 247 on an oral and a skin microbiome dataset from qiita (Supplementary Table 1, bottom). Consistent
 248 with the performance on gut microbiome datasets, although the difference in median variance is small
 249 (Supplementary Figure 2), GMPR achieves the lowest rank for majority of the OTUs, followed by CSS
 250 (Figure 7).

251 **Real data: GMPR improves the reproducibility of normalized abundances**

252 When replicates are available, we could evaluate the performance of normalization based on its ability to
 253 reduce between-replicate variability. Normalization will increase the reproducibility of the normalized
 254 OTU abundances. In this section, we compare the performance of different normalization methods based
 255 on a reproducibility analysis of a fecal stability study, which aims to compare the temporal stability of
 256 different stool collection methods (Sinha et al., 2016). In this study, 20 healthy volunteers provided the
 257 stool samples and these samples were subject to different treatment methods. The stool samples were
 258 then frozen immediately or after storage in ambient temperature for one or four days for the study of
 259 the stability of the microbiota. Each sample had two to three replicates for each condition and thus we
 260 could perform reproducibility analysis based on the replicate samples. We evaluate the reproducibility
 261 for the “no additive” treatment method for the data generated at Knight lab (Sinha et al., 2016), where
 262 the stool samples were left untreated. Under this condition, certain bacteria will grow in the ambient
 263 temperature with varying growth rates and we thus expect a lower agreement between replicates after
 264 four-day ambient temperature storage.

We conduct the reproducibility analysis on the core genera, which are present in more than 75%
 samples (a total of 26 genera are assessed). We first estimate the size factors based on the OTU-level
 data and the genus-level counts are divided by the size factors to produce normalized genus-level
 abundances. Intraclass correlation coefficients (ICC) is used to quantify the reproducibility for the

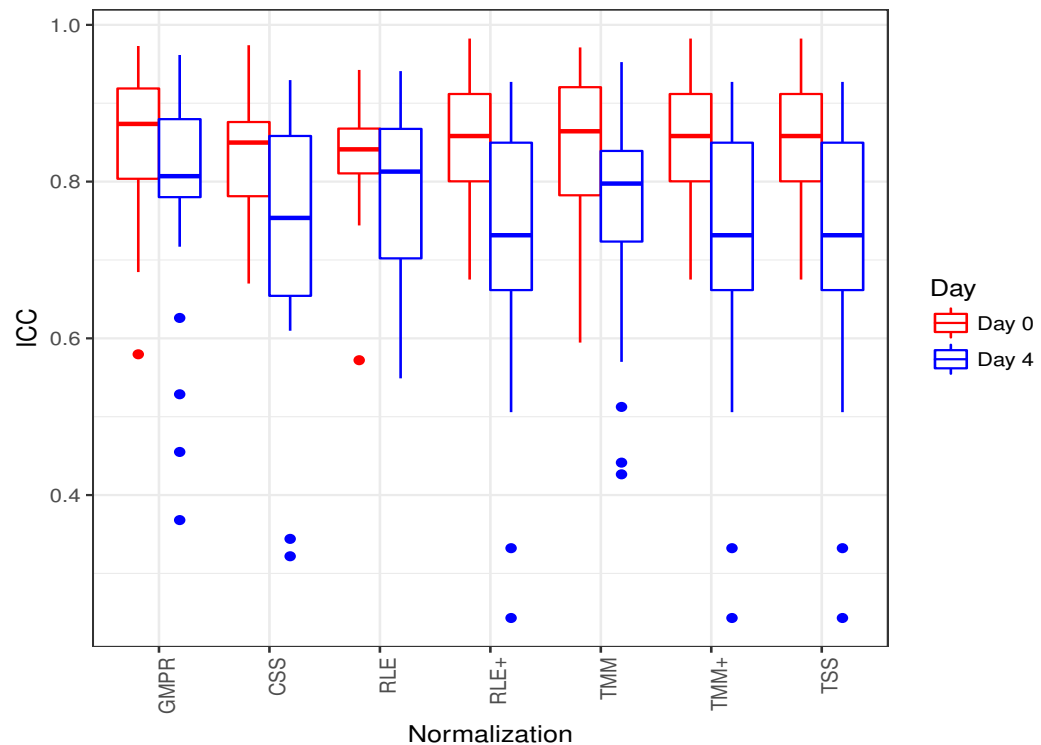


Figure 8. ICC as a measurement for reproducibility is calculated for 26 core genera normalized by different methods for “day 0” and “day 4” respectively.

genus-level normalized abundances. The ICC is defined as,

$$\rho = \frac{\sigma_b^2}{\sigma_b^2 + \sigma_\varepsilon^2}$$

265 where σ_b^2 represents the biological variability, i.e., sample-to-sample variability and σ_ε^2 represents the
 266 replicate-to-replicate variability. We calculate the ICC for 26 core genera for “day 0” (immediately frozen)
 267 and “day 4” (frozen after four-day storage) respectively. The ICCs are estimated using the R package
 268 “ICC” based on the mixed effects model. An ICC closer to one indicates excellent reproducibility.

269 Figure 8 shows that the reproducibility of the genera in “day 0” has higher reproducibility than “day
 270 4” regardless of the normalization method used since reproducibility decreases as certain bacteria grow
 271 randomly as time elapses. While all the methods have resulted in comparable ICCs for “day 0”, GMMPR
 272 achieves higher ICCs for “day 4” than the rest methods. Sinha et al. (2016) showed that most taxa were
 273 relatively stable over 4 days and only a small group of taxa (mostly OTUs from *Gammaproteobacteria*)
 274 displayed a pronounced growth at ambient temperature. This suggests that most of the genera may be
 275 temporally stable and their “day 4” ICCs should be close to the “day 0” ICCs. However, due to the
 276 compositional effect, if the data are not properly normalized, a few fast-growing bacteria will skew the
 277 relative abundances of other bacteria, leading to apparently lower ICCs for those stable genera. In contrast,
 278 the GMMPR method is more robust to differential or outlier taxa as demonstrated by the simulation study,
 279 which explains higher ICCs for “day 4” samples.

280 CONCLUSION AND DISCUSSION

281 Normalization is a critical step in processing microbiome data, rendering multiple samples comparable by
 282 removing the bias caused by variable sequencing depths. Normalization paves the way for the downstream
 283 analysis, especially for differential abundance analysis of microbiome data, where proper normalization
 284 could reduce the false positive rates due to compositional effects. However, the characteristics of

285 microbiome sequencing data, including over-dispersion and zero-inflation, make the normalization a
286 non-trivial task.

287 In this study, we propose the GMPR method for normalizing microbiome sequencing data by address-
288 ing the zero-inflation. In one simulation study, we demonstrate GMPR's effectiveness by showing it
289 performs better than other normalization methods in recovering the original library sizes when a subset
290 of OTUs are differentially abundant or when random outlier OTUs exist. In another simulation study,
291 GMPR yields better FDR control and higher power in detecting differentially abundant OTUs. In real data
292 analysis, we show GMPR reduces the inter-sample variability and increases inter-replicate reproducibility
293 of normalized taxa abundances. Overall, GMPR outperforms RNA-Seq normalization methods including
294 TMM and RLE and modified TMM+ and RLE+. It also yields better performance than CSS, which is a
295 normalization method specifically designed for microbiome data. As a general normalization method for
296 zero-inflated sequencing data, GMPR could also be applied to other sequencing data with excessive zeros
297 such as single-cell RNA-Seq data (Vallejos et al., 2017).

298 We note that the main application of GMPR method is for taxon-level analysis such as the presented
299 differential abundance analysis and reproducibility analysis, where it is important to distinguish those
300 "truly" differential from "falsely" differential taxa due to compositional effects. Although we could apply
301 the proposed normalization to (weighted) distance-based statistical methods such as ordination, clustering
302 and PERMANOVA (Caporaso et al., 2010; Chen et al., 2012) based on the GMPR-normalized abundance
303 data, simulations show that the advantage of using GMPR is very limited for such applications, compared
304 to the traditionally used TSS method (i.e., proportion-based method) (Supplementary Figure 3). This
305 is explained by the fact that the distance-based analysis focuses on the overall dissimilarity and the
306 proportional data is already efficient enough to capture the overall dissimilarity. Probably, more important
307 factors to consider in distance-based statistical methods are the selection of the most relevant distance
308 measure and/or the application of appropriate transformation after normalization (Costea et al., 2014;
309 Thorsen et al., 2016).

310 Besides the size factor-based approach (GMPR, CSS, TSS, RLE, TMM), the other popular approach
311 for normalizing the microbiome data is through rarefaction. Both approaches have weakness and
312 strength for particular applications. Although rarefaction discards a significant portion of the reads and
313 is probably not optimal from an information perspective, it is still widely used for microbiome data
314 analysis, particularly for α - and β -diversity analysis. The reason for its extensive use is that the majority
315 of the taxa in the microbiota are of low abundance and their presence/absence strongly depends on the
316 sequencing depth. Thus rarefaction puts the comparison of α - and β -diversity on an equal basis. Size
317 factor-based normalization, on the other hand, is unable to address this problem. Thus rarefaction is still
318 recommended for α - and β -diversity analysis, especially for unweighted measures and for confounded
319 scenarios, where the sequencing depth correlates with the variable of interest (Weiss et al., 2017). For
320 differential abundance analysis, one major challenge is to address the compositional problem. Rarefaction
321 has a limited ability in this regard since the total sum constraint still exists after rarefaction. In addition, it
322 suffers from a great power loss due to the discard of a large number of reads (McMurdie and Holmes,
323 2014). In contrast, the size factor-based approaches are capable of capturing the invariant part of the taxa
324 counts and address the compositional problem efficiently through normalization by the size factors. The
325 size factors could be naturally included as offsets in count-based parametric models to address uneven
326 sequencing depth (Chen et al., 2018).

327 GMPR is an inter-sample normalization method and has a computational complexity of $O(n^2q)$, where
328 n and q are the number of samples and features respectively. While GMPR calculates the size factors
329 for a typical microbiome dataset ($n < 1000$) in seconds, it does not scale linearly with the sample size.
330 Large samples sizes are increasingly popular for epidemiological study and genetic association study of
331 the microbiome (Robinson et al., 2016; Hall et al., 2017), where tens or hundreds of thousands of samples
332 will be collected to detect weak association signals. For such large sample sizes, GMPR may take a much
333 longer time. A potential strategy for efficient computation under ultra-large sample sizes is to divide the
334 dataset into overlapping blocks, calculate GMPR size factors on these blocks and unify the size factors
335 through the overlapping samples between blocks. To increase the computational efficiency of GMPR for
336 ultra-large sample sizes will be the focus of our future research.

337 REFERENCES

- 338 Aird, D., Ross, M. G., Chen, W.-S., Danielsson, M., Fennell, T., Russ, C., Jaffe, D. B., Nusbaum, C., and
339 Gnirke, A. (2011). Analyzing and minimizing pcr amplification bias in illumina sequencing libraries.
340 *Genome Biol*, 12(2):R18.
- 341 Anders, S. and Huber, W. (2010). Differential expression analysis for sequence count data. *Genome Biol.*,
342 11(10):R106.
- 343 Caporaso, J. G., Kuczynski, J., Stombaugh, J., Bittinger, K., Bushman, F. D., Costello, E. K., Fierer, N.,
344 Peña, A. G., Goodrich, J. K., Gordon, J. I., Huttley, G. A., Kelley, S. T., Knights, D., Koenig, J. E.,
345 Ley, R. E., Lozupone, C. A., McDonald, D., Muegge, B. D., Pirrung, M., Reeder, J., Sevinsky, J. R.,
346 Turnbaugh, P. J., Walters, W. A., Widmann, J., Yatsunencko, T., Zaneveld, J., and Knight, R. (2010).
347 Qiime allows analysis of high-throughput community sequencing data. *Nat Methods*, 7(5):335–6.
- 348 Chen, J., Bittinger, K., Charlson, E. S., Hoffmann, C., Lewis, J., Wu, G. D., Collman, R. G., Bushman,
349 F. D., and Li, H. (2012). Associating microbiome composition with environmental covariates using
350 generalized unifracs distances. *Bioinformatics*, 28(16):2106–13.
- 351 Chen, J., King, E., Deek, R., Wei, Z., Yu, Y., Grill, D., and Ballman, K. (2018). An omnibus test for
352 differential distribution analysis of microbiome sequencing data. *Bioinformatics*, 34(4):643–51.
- 353 Chen, J. and Li, H. (2013). Variable selection for sparse dirichlet-multinomial regression with an
354 application to microbiome data analysis. *Ann. Appl. Stat.*, 7(1).
- 355 Costea, P. I., Zeller, G., Sunagawa, S., and Bork, P. (2014). A fair comparison. *Nat Methods*, 11(4):359.
- 356 Dillies, M.-A., Rau, A., Aubert, J., Hennequet-Antier, C., Jeanmougin, M., Servant, N., Keime, C., Marot,
357 G., Castel, D., Estelle, J., Guernec, G., Jagla, B., Jouneau, L., Laloë, D., Le Gall, C., Schaëffer, B.,
358 Le Crom, S., Guedj, M., Jaffrézic, F., and French StatOmique Consortium (2013). A comprehensive
359 evaluation of normalization methods for illumina high-throughput rna sequencing data analysis. *Brief*
360 *Bioinform*, 14(6):671–83.
- 361 Fortin, J., Labbe, A., Lemire, M., Zanke, B., Hudson, T., and Fertig, E. (2014). Functional normalization
362 of 450k methylation array data improves replication in large cancer studies. *Genome Biol.*, 15(11):503.
- 363 Hall, A. B., Tolonen, A. C., and Xavier, R. J. (2017). Human genetic variation and the gut microbiome in
364 disease. *Nat Rev Genet*, 18(11):690–699.
- 365 Li, P., Piao, Y., Shon, H. S., and Ryu, K. H. (2015). Comparing the normalization methods for the
366 differential analysis of illumina high-throughput rna-seq data. *BMC Bioinformatics*, 16:347.
- 367 Love, M. I., Huber, W., and Anders, S. (2014). Moderated estimation of fold change and dispersion for
368 rna-seq data with deseq2. *Genome Biol*, 15(12):550.
- 369 Mandal, S., Van Treuren, W., White, R. A., Eggesbø, M., Knight, R., and Peddada, S. D. (2015). Analysis
370 of composition of microbiomes: a novel method for studying microbial composition. *Microb Ecol*
371 *Health Dis*, 26(1):27663.
- 372 McMurdie, P. J. and Holmes, S. (2014). Waste not, want not: why rarefying microbiome data is
373 inadmissible. *PLoS Comput Biol*, 10(4):e1003531.
- 374 Morton, J. T., Sanders, J., Quinn, R. A., McDonald, D., Gonzalez, A., Vázquez-Baeza, Y., Navas-Molina,
375 J. A., Song, S. J., Metcalf, J. L., Hyde, E. R., Lladser, M., Dorrestein, P. C., and Knight, R. (2017).
376 *mSystems*, 2(1):e00162–16.
- 377 Paulson, J., Stine, O., Bravo, H., and Pop, M. (2013). Differential abundance analysis for microbial
378 marker-gene surveys. *Nat. methods*, 10(12):1200–1202.
- 379 Robinson, C. K., Brotman, R. M., and Ravel, J. (2016). Intricacies of assessing the human microbiome in
380 epidemiologic studies. *Ann Epidemiol*, 26(5):311–21.
- 381 Robinson, M. D., McCarthy, D. J., and Smyth, G. K. (2010). edgeR: a bioconductor package for differential
382 expression analysis of digital gene expression data. *Bioinformatics*, 26(1):139–40.
- 383 Robinson, M. D. and Oshlack, A. (2010). A scaling normalization method for differential expression
384 analysis of rna-seq data. *Genome Biol.*, 11(3):R25.
- 385 Sinha, R., Chen, J., Amir, A., Vogtmann, E., Shi, J., Inman, K. S., Flores, R., Sampson, J., Knight, R., and
386 Chia, N. (2016). Collecting fecal samples for microbiome analyses in epidemiology studies. *Cancer*
387 *Epidemiol Biomarkers Prev*, 25(2):407–16.
- 388 Thorsen, J., Brejnrod, A., Mortensen, M., Rasmussen, M. A., Stokholm, J., Al-Soud, W. A., Sørensen,
389 S., Bisgaard, H., and Waage, J. (2016). Large-scale benchmarking reveals false discoveries and count
390 transformation sensitivity in 16s rna gene amplicon data analysis methods used in microbiome studies.
391 *Microbiome*, 4(1):62.

- 392 Tsilimigras, M. C. and Fodor, A. A. (2016). Compositional data analysis of the microbiome: fundamentals,
393 tools, and challenges. *Ann Epidemiol*, 26(5):330–5.
- 394 Vallejos, C. A., Risso, D., Scialdone, A., Dudoit, S., and Marioni, J. C. (2017). Normalizing single-cell
395 rna sequencing data: challenges and opportunities. *Nat Methods*, 14(6):565–571.
- 396 Wang, Z., Gerstein, M., and Snyder, M. (2009). Rna-seq: a revolutionary tool for transcriptomics. *Nat*
397 *Rev Genet*, 10(1):57–63.
- 398 Weiss, S., Xu, Z. Z., Peddada, S., Amir, A., Bittinger, K., Gonzalez, A., Lozupone, C., Zaneveld, J. R.,
399 Vázquez-Baeza, Y., Birmingham, A., Hyde, E. R., and Knight, R. (2017). Normalization and microbial
400 differential abundance strategies depend upon data characteristics. *Microbiome*, 5(1):27.
- 401 Wu, G. D., Chen, J., Hoffmann, C., Bittinger, K., Chen, Y. Y., Keilbaugh, S. A., Bewtra, M., Knights, D.,
402 Walters, W. A., Knight, R., Sinha, R., Gilroy, E., Gupta, K., Baldassano, R., Nessel, L., Li, H., Bushman,
403 F. D., and Lewis, J. D. (2011). Linking long-term dietary patterns with gut microbial enterotypes.
404 *Science*, 334(6052):105–108.